Journal of Environmental Management 323 (2022) 116219

Contents lists available at ScienceDirect

Journal of Environmental Management

journal homepage: www.elsevier.com/locate/jenvman

Research article

Priority setting for restoration in surrounding savannic areas of the Brazilian Pantanal based on soil loss risk and agrarian structure

Rômullo O. Louzada [a,*], Ivan Bergier [b,c], Juliana M.F.de S. Diniz [d], A. Guerra [e], Fábio de O. Roque [a,f]

[a] Programa de Pós-Graduação em Ecologia e Conservação, Universidade Federal de Mato Grosso do Sul, Campo Grande, Brazil
[b] Embrapa Pantanal, Corumbá, Brazil
[c] Embrapa Agricultura Digital, Campinas, Brazil
[d] Instituto Nacional de Pesquisas Espaciais, São José dos Campos, Brazil
[e] Instituto Homem Pantaneiro, Corumbá, Brazil
[f] Centre for Tropical Environmental and Sustainability Science and College of Science and Engineering, James Cook University, Cairns, Queensland, Australia

ARTICLE INFO

Keywords:
Agrarian structure
Check dams
Gullies
Palisades
Soil erosion
USLE

ABSTRACT

Soil health is at the core of the sustainability agenda. As in many agroecosystems in the tropics, soil erosion is a major issue in poorly managed pasturelands. A noteworthy case is located in the Upper Taquari River Basin (UTRB), as part of the Upper Paraguay Basin on the plateau with drainage waters for the Taquari megafan in the Brazilian Pantanal. Here we combine slope (S-factor), erodibility (E-factor), rainfall-rainy day ratio (R-factor), and vegetation and soil indices (C-factor) to locate erosion risk and prioritize eco-engineering interventions via palisades and small dams in UTRB. The method consisted of assessing distinct weights between Universal Soil Loss Equation (USLE) factors in a GIS platform, providing 35 combinations of classes as low, moderate, high, and very high erosive risk. The validation of the method was based on the ravine and plain ground truths obtained from high-resolution raster data. The best weight of USLE factors aids to locate critical erosive sites and vegetation patterns. Then, erosion risk and interventions were analyzed according to land use and rural property sizes in the government's Rural Environmental Registry (CAR) database. Overall, the natural factors of slope and erodibility in a proportion of 25% and 75% in GIS algebra provided the best mapping accuracy result. About 65% of the UTRB has high or very high erosion risks, and 70% of the available area can be acknowledged as degraded pasturelands. A total of 4744 erosion interventions were recorded, with an accuracy of 65.28% and 61.15% for check dams and palisades interventions, respectively. The number of necessary interventions in areas of native vegetation was almost 50% higher than in pasturelands. Even though micro landowners occupy most of the watershed, large properties have about ten times as many areas at high risk of erosion. The mutual cooperation between properties, independently of size, is supported by governmental public policies like incentives for ecosystem services restoration of critical gullies, with CAR compliance and fiscalization.

1. Introduction

Soil erosion is an important issue in implementing a Global Sustainable Agenda (Wuepper et al., 2020). Decreasing land degradation responds positively to six of seventeen UN Sustainable Development Goals (Keesstra et al., 2016). Eroded soils provide ecosystem disservices that refute their natural capital stocks (Dominati et al., 2010). The impact for landowners is direct, given the need for nonrenewable resources for maintaining agricultural production (Telles et al., 2013), but also indirect and cumulative for society due to loss of biodiversity and ecosystem services of support and regulation (García-Ruiz et al., 2017). Land use intensification scenarios associated with climate change estimate erosion rate growth of up to 66% by 2070 worldwide (Borrelli et al., 2020).

Agricultural countries in tropical regions invariably perceive soil loss as an unsolved task. For instance, Wuepper et al. (2020) put Brazil on the top shelf of soil loss at around 4 t ha^{-1} yr^{-1}, almost twice the global average of 2.4 t ha^{-1} yr^{-1}. Mapping active erosive features (Senanayake et al., 2020) or the location of interventions in severe erosions (Pourghasemi et al., 2020) are issues for conservation and food security,

* Corresponding author.
E-mail address: romullo_louzada@yahoo.com.br (R.O. Louzada).

https://doi.org/10.1016/j.jenvman.2022.116219
Received 24 June 2022; Received in revised form 5 September 2022; Accepted 6 September 2022
Available online 12 September 2022

where GIS and RS are widely applied (Sepuru and Dube, 2018). Spatialization makes it possible to plan mitigating actions and reduce impacts on and off-site (Boardman et al., 2019). At the landscape scale, the rate of soil erosion is critical for the quantitative assessment of land degradation (Abdulkareem et al., 2019). Models are the most appropriate tools for simulating soil erosion at a relatively large spatial scale (Gao and Wang, 2019). Among the most widely used, the Universal Soil Loss Equation (USLE), developed by Wischmeier and Smith (1965) for agricultural sites in the United States, remains valid and commonly applied around the world to assess gross erosion or disaggregated soil sediments in plots (Alewell et al., 2019).

Much of such success of USLE is due to the ease of estimating factors influencing erosion, such as relief, soil erodibility, rainfall erosivity, and land use or cover changes, both by remote sensing data (RS) and data layers within the Geographical Information System (GIS) platforms (Pruski, 2006). In this sense, RS with GIS techniques allows demonstrating a quali-qualitative picture of the risk of soil loss, broadening the view on the management of natural resources (Yesuph and Dagnew, 2019). Despite the robustness of mathematical erosion prediction models, there is still room for uncomplex layer algebra techniques for the erosion risk dimension (Ewunetu et al., 2021), which is very appropriate for decision makers to flash allocation of resources for local restoration (Pena et al., 2020).

Spatialization of active erosive alone is not enough for setting priorities for restoration. Although there have been significant advances in increasing ecological resilience on a large scale (Beller et al., 2019), landscape restoration projects need to incorporate socioeconomic dimensions, such as governance, social-political, and financial constraints, and agrarian structure because they are key determinants of restoration success (Armsworth, 2014).

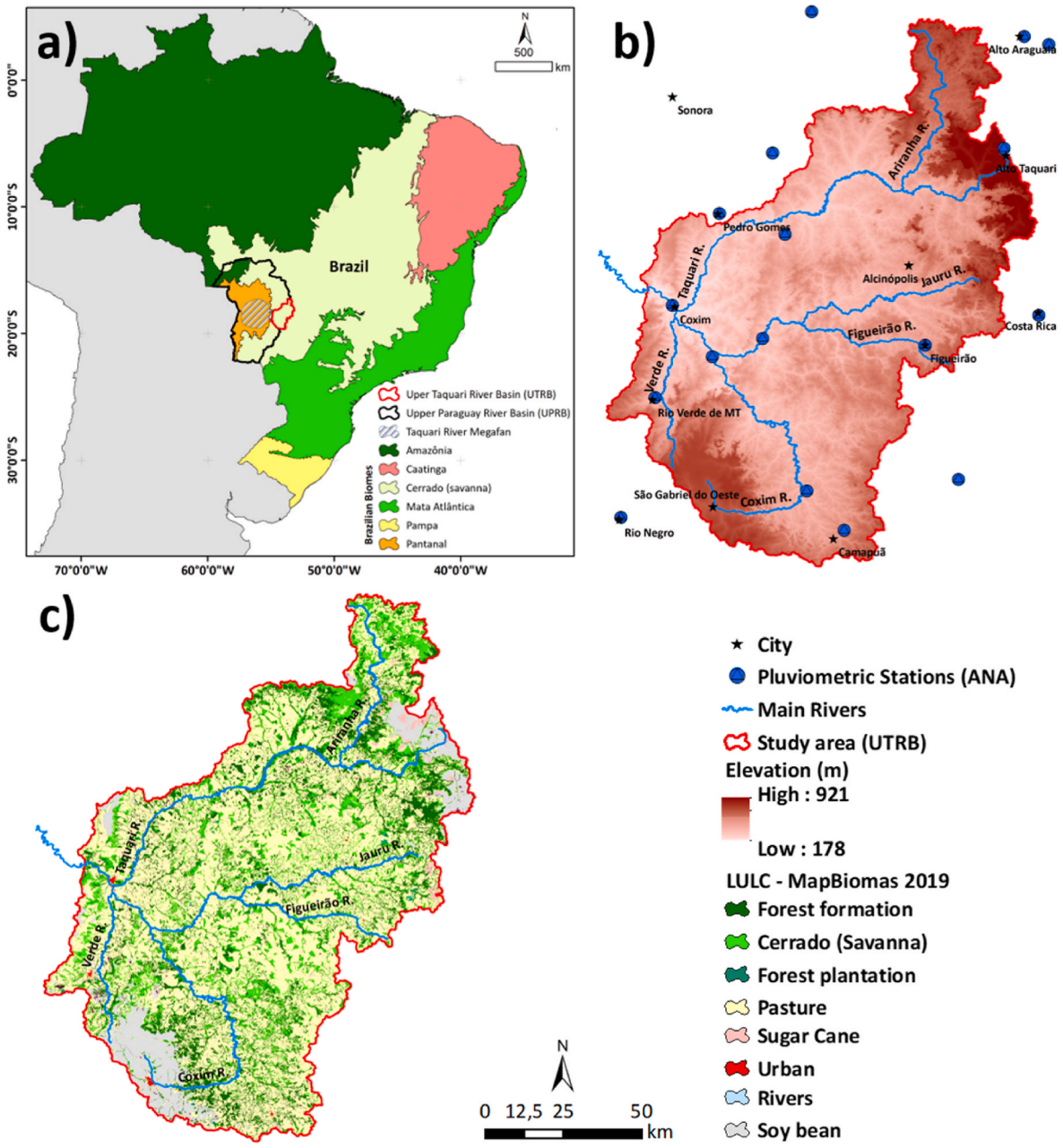

Fig. 1. Location of the Upper Taquari River Basin. (a) official map of Brazilian biomes with emphasis on the UTRB as part of the UPRB and located in the Cerrado, as well as the Taquari megafan in the Pantanal; (b) cities, main rivers of UTRB and rainwater stations of "Agência Nacional das Águas - ANA" used to calculate the rainfall index (item 2.2.1), overlaid by DEM ALOS-PALSAR (item 2.2.3); (c) Land Use/Land Cover from MapBiomas project of 2019 (Souza et al., 2020).

Here we use a highly tropical eroded area around the Pantanal, the biggest continuous wetland in the world, as an example to apply a multi-criteria approach based on USLE parameters on a GIS and RS that identifies priority areas at risk of soil loss and land restoration, including drainage criteria from high-resolution RS, through small dams and palisade interventions. Furthermore, we analyze the agrarian structure of the region and discuss possible solutions to mitigate the problem based on the fact that the real agents are the rural landowners. We choose the noteworthy Upper Taquari River Basin (UTRB) as a study case because this region has experienced rapid land cover clearance over the last 30 years (Roque et al., 2016). Gigatonnes of topsoil layers have been transported to the Pantanal by uncontrolled runoff, conjointly with the loss of invaluable biodiversity (Bergier, 2013; Lo et al., 2022). As climate changes may alter rainfall and droughts patterns in the Pantanal watersheds (Thielen et al., 2020), one can expect an increase in summer river runoff and sediment load to the plains (Bergier et al., 2018), and an increase in winter wildfire recurrence, both adversely affecting Pantanal's biodiversity and ecological functioning (Silva et al., 2019; Libonati et al., 2020). For the sediment load, Colman et al. (2019) pointed to up to 40% increased soil loss by 2050 from land-use changes, accompanied by on-site (UTRB) and off-site (Pantanal) pesticide inputs (Roque et al., 2021), and a greater probability of river avulsions of the Taquari River in lowlands (Bergier et al., 2018; Louzada et al., 2020, 2021).

2. Material and methods

2.1. Study area

As an important watershed of the Upper Paraguay River Basin (UPRB), the Upper Taquari River Basin (UTRB) covers 28,111 km^2 of the states of Mato Grosso and Mato Grosso do Sul in the central-western region of Brazil, bounded by latitudes 17°30′S to 19°30′S and longitudes 53°00′W to 55°00′W (Fig. 1). The elevation ranges from 178 to 921 m above sea level. In general, the relief is a mosaic of depressions, isolated planes, and elongated plateaus, highlighting the Maracaju plateau near the city of Coxim, which shares the plateau with the Pantanal (plain). The rivers of the UTRB are geologically stable through bedrocks, but connected to unstable alluvial systems in the Pantanal wetland (Assine, 2005). The systematic decrease in the longitudinal gradient in the Pantanal associated with the high sediment load of the uplands determined one of the most notable depositional systems in the world, the Taquari megafan (Assine, 2005).

A large part of the UTRB soils originates from sedimentary rocks. Therefore, it presents deep horizons with sandy texture and low natural fertility (Galdino et al., 2005). In terms of precipitation, the summer rainy season runs from November to March (Marengo et al., 2015), ranging from 1700–1,800 mm in the extreme NE to 1,200 mm in the S and SW regions (Thielen et al., 2020). Regarding vegetation and land use, the original formation of the Cerrado (Brazilian savanna) was gradually replaced by grazing on sandy soils and agriculture on clay soils after the 1970s (Galdino et al., 2005; Souza et al., 2020).

2.2. Soil erosion risk

The erosion process can be suitably represented and modeled in the GIS environment (El Jazouli et al., 2017). Here, we apply the USLE logic with other principles of geospatial analysis on ArcGIS® version 10.4.1. In the original equation of USLE, $A = RKLSCP$, where R is erosivity from rainfall, K is soil erodibility, LS is the topographic factor, and C and P refer to cover and management. Our set of factors preserved only the erodibility factor (E), replacing the original elements of the USLE, such as rainfall index (R), slope (S), and the best vegetation index (C). Here, conservation practices corresponding to the P-factor were excluded from the multicriteria analysis due to missing updated data. Thus, our final equation was *Erosion risk* = *RESC*, whose weights for each variable are established in item 2.3.

2.2.1. Rainfall index (R)

In tropical regions, precipitation is the most important driver of the erosive process. Summer heavy rains have been more frequent in the last decade in the UTRB (Bergier et al., 2018; Thielen et al., 2020). Thus, we consider the method of Bergier et al. (2018) more relevant to compose the R factor as it calculates the rain index as a simple ratio of historical total precipitation in mm to the sum of rainy days. The data were collected at ANA pluviometric stations available in the hidroweb (https://www.snirh.gov.br/hidroweb/). A total of 21 stations were selected (see Fig. 1b) based on location criteria, within or within 50 km of the UTRB seeking to fill the entire study area. The results of the ratio are shown in Supplementary Material (see Table S1). The R factor as raster data was prepared by kriging available on ArcGIS spatial analyst tools applying the default parameters across the watershed boundaries.

2.2.2. Soil erodibility (E)

The spatialization of soil erodibility was based on the recent review of the theme by Godoi et al. (2021) using multilayer soil properties in a cell size of 250 m.

2.2.3. Slope (S)

The topographic slope factor was generated from DEM of ALOS-PALSAR images, specifically, the radiometric terrain corrected by resampling of SRTM with a spatial resolution of 12.5 m (Laurencelle et al., 2015), available at (https://search.asf.alaska.edu/#/). Table S2 shows the list of scenes for the DEMs mosaic (Fig. 1b) and slope (S).

2.2.4. Land Use/Land Cover (C)

Land use and land cover generally vary with the seasons. This is the case of agriculture, whose planting of grains in Brazil has, on average, two harvests interspersed with a fallow period to control Asian soybean rust, which lasts from June to September in the Cerrado biome (Seixas and Godoy, 2007). During these months, the soil is exposed to runoff but that practice is made at the apex of the dry season, which would wrongly entail potential erosive risk. In this sense, the vegetation indices of orbital images are useful to extract seasonal surface features to calculate the C factor in the USLE (see applications in Durigon et al., 2014; Chen et al., 2019).

Here, we tested eight vegetation and soil indices two times (Table 1), September 2020 (dry) and April 2021 (wet-dry transition) using Sentinel-2A Level 2 data available from the European Space Agency. For the calculations, we use the SNAP software version 8.0.0 (https://step.esa.int/) on spectral bands green (G), red (R), and near-infrared (NIR)

Table 1
List of vegetation and soil radiometric indices applied to the calculation of C. factor.

Type	Index	Equation	Reference
Vegetation	Normalized Difference Vegetation Index (NDVI)	*(NIR - R)/(NIR + R)*	Rouse et al. (1973)
	Transformed Normalized Difference Vegetation Index (TNDVI)	*sqrt((NIR - R)/(NIR + R) + 0.5)*	Senseman et al. (1996)
	Enhanced Vegetation Index (EVI)	*2.4 * (NIR - R)/(NIR + R + 1)*	Jiang et al. (2008)
	Soil Adjusted Vegetation Index (SAVI)	*(1 + L) * (NIR - R)/(NIR + R + L)*	Huete (1988)
	Transformed Soil Adjusted Vegetation Index (TSAVI)	*s * (NIR - s * R - a)/(s * NIR + R - a * s + X * (1 + s^2))*	Baret and Guyot (1991)
	Modified Soil Adjusted Vegetation Index (MSAVI)	*(1 + Z) * (NIR - R)/(NIR + R + Z)*	Qi et al. (1994)
Soil	Brightness Index (BI)	*sqrt((R^2) + (G^2)/2)*	Mathieu et al. (1998)
	Colour Index (CI)	*(R - G)/(R + G)*	Escadafal (1989)

with a pixel resolution of 10 m.

Terms of the above equations. SAVI: L is the adjustment factor; TSAVI: *a* is the soil line intercept; *s* is the soil line slope; *X* is the adjustment factor to minimize soil noise. For MSAVI, the Z is calculated by (1–2 * NDVI * s * (NIR - s * R), where *s* is the soil line slope.

The process of choosing the best date and index to obtain the C factor was based on the comparison of the difference of the means between samples of a gully (high risk), obtained at a scale of 1:10,000 of the high-resolution base map ArcGIS, and the opposite flat relief (low risk), with agricultural areas practice (Fig. S1 in Supplementary Material). Besides, the Sentinel-2 scenes were used to replicate the method and compose the *C-factor* mosaic in the UTRB according to the two possibilities of date imagery (all scenes and multispectral bands information are shown in Table S3).

2.3. Multicriteria analysis and validation

Before multicriteria analysis, spatial factors were resampled to the same 10 m *C-factor* resolution. The natural breaking method was applied in the reclassification of all rasters (Gao and Wang, 2019), as low risk of erosion (class 1), moderate (class 2), high (class 3), and very high risk of soil erosion (class 4).

In this study, we evaluated the importance of each factor using weights in the raster calculation tools. Thus, a set of possibilities was derived by considering an increase of 25% in the factor, hence totalizing 35 tests (Table 2).

To validate the maps, we preserved the method of comparison of eroded to non-eroded themes in item 2.2.4., including 2 preserved flats sites and 32 gullies spatialized in the UTRB (see examples in Fig. S2). The selection was done by the average percentage of pixels in class 4 (very high) expected for gullies and class 1 (low) for flat sites. The locations of all validation samples in the UTRB are exhibited in Fig. S3 of the Supplementary Material.

2.4. Locations for intervention

An effective gully recovery scheme should consider vegetative, edaphic, and mechanical techniques (Machado et al., 2006), especially on fragile soils primarily composed of sand (Filizola et al., 2011). For quick mitigation of soil losses, we evaluate the best location of recovery techniques for gullies. Hence, the methods of intervention were based on principles of ecohydrology or eco-engineering (e.g., low landscape impacts, organic and in situ materials), in contrast to classical civil engineering (Norris et al., 2008). Within the scope of techniques, we evaluated the palisades represented by perpendicular posts of bamboo or *Eucalyptus* sp. wood installed on sloping lands, which previously have shown promising results (Tardio et al., 2017; Rodrigues, 2018). Likewise, checking (small) dams through the soil, sandbags, or stone lines in the gullies' bed have been effective in reducing stream flow (Xu et al., 2020).

To determine the points suitable for palisades and check dams, firstly we vectored all drainage lines in the UTRB in a similar way to gully samples. In total, 31,413 drainages were identified (see Fig. S3 on the Supplementary Material). This step was necessary because ANA's official watercourses are incomplete, displaced, and do not include erosions' ramifications. Palisades were calculated by transforming the starting line into a point, then selecting only combined points in class 4 that pixels are in the appropriate erosion risk test. To avoid false positives, we added another layer of exclusion based on thresholds of the 2019 map of Mapbiomas of savanna and forest formation, which was derived from one of the land use factors in Table 1 that were not applied in the assessment tests.

For check dams, we analyzed the distribution of drainage length in gullies samples, looking for lines in a range equal to the last quartile of erosion lines. The results showed that 22,313 features had an equivalent length (123 m–1,623 m). In hydrographic basins, the main trunk river is the regional base level. For ravines, the bed is also expected to be at the local minimum, hence an adequate point of sediment impoundment. Sequentially, the nodules of the lines were changed to points with the selection clause where once again lines overlapped by class 4, excluding the points of the palisades and the same vegetation thresholds.

The assessment of eco-engineering interventions was also referenced in the high-resolution image from the base map plugin of the ArcGIS. Using a simple random points sampler, with a 95% confidence interval, at a minimum distance of 1 km, it was possible to visually inspect whether palisades and check dams were in erosion (valued 1) or not (valued 0).

2.5. Exploratory analysis of the forest code CAR data

The degree of compliance with environmental legislation on farms, established by the Brazilian Forest Code (Law 12,651/2012), is precisely linked to the size of the property (Stefanes et al., 2018). Thus, we searched for the Rural Environmental Registry (CAR) database available on the SICAR website (https://www.car.gov.br/publico/imoveis/index), which gathers the main attributes of rural properties, to support a conservation action prioritization plan at the farm scale. Here, we selected the layers of: i) total area; ii) Legal Reserve (RL) area with a minimum of 20% of native vegetation; iii) permanent preservation area (APP) that represents the riparian watercourse; and iv) unrestricted or consolidated area (AC) for economic activities, mainly as providing services of food (meat/grain), timber/fiber (planted wood) and liquid biofuels (sugarcane/grain). An example of layers of property is shown in Fig. S4.

The polygons of properties were divided into four categories according to the Forest Code: micro (0–4 modules), small (4–10 modules), medium (10–20 modules), and large (above 20 modules). The modules vary according to the size of the municipality, for which ranges were arbitrarily chosen except for the first category (up to four modules) belonging to a general rule of the forest code for special APP size treatments.

3. Results

3.1. Suitable C-factor

The gully and the flat terrain are close together and located in the same Sentinel-2 scene, therefore sharing the same weather conditions.

Table 2
Algebra map scheme to calculate soil erosion risk tests. In correspondence to the original USLE elements, S is the topographical factor, E is the soil erodibility, R represents the rainfall index factor and C is the land use/land cover factor.

Test	Algebraic model	Test	Algebraic model	Test	Algebraic model	Test	Algebraic model	Test	Algebraic model
1	S1	8	S0.5 + E0.25 + R0.25	15	S0.25 + E0.5 + C0.25	22	E0.75 + R0.25	29	E0.25 + R0.75
2	S0.75 + E0.25	9	S0.5 + E0.25 + C0.25	16	S0.25 + E0.25 + R0.5	23	E0.75 + C0.25	30	E0.25 + C0.75
3	S0.75 + R0.25	10	S0.5 + R0.25 + C0.25	17	S0.25 + E0.25 + C0.5	24	E0.5 + R0.5	31	R1
4	S0.75 + C0.25	11	S0.25 + E0.75	18	S0.25 + R0.5 + C0.25	25	E0.5 + C0.5	32	R0.75 + C0.25
5	S0.5 + E0.5	12	S0.25 + R0.75	19	S0.25 + R0.25 + C0.5	26	E0.5 + R0.25 + C0.25	33	R0.5 + C0.5
6	S0.5 + R0.5	13	S0.25 + C0.75	20	S0.25 + E0.25 + R0.25 + C0.25	27	E0.25 + R0.5 + C0.25	34	R0.25 + C0.75
7	S0.5 + C0.5	14	S0.25 + E0.5 + R0.25	21	E1	28	E0.25 + R0.25 + C0.5	35	C1

In addition, their sizes are equivalent, with 5.73 ha (576 pixels) for the canyon and 5.34 ha for the plain (538 pixels). Here, we assume the indices are positive and closer to the maximum for photosynthetically active vegetation. In this case, it resembles grasses or plantations in the flat relief area, while in the exposed soil of the gully the values tend to be much lower. The means of indices from the dry period (September 2020), and the transition of wet/dry (April 2021) are shown in Table 3. The vegetation indices for April 2021 were more consistent regarding the differentiation premise between healthy vegetation and exposed soil. In general, the indices presented similar results, but the MSAVI factor was chosen to compose the *C-factor* because it overlaps the others on differences between the antagonistic areas.

3.2. Maps of soil erosion risk in UTRB

The Rainfall Index (*R*), Soil erodibility (*E*), Slope (*S*), and Land Use/Land Cover (*C*) factors are shown in Fig. 2. The *R* data, derived from the ANA database, showed a coefficient of variation CV = 8.9%, in which the first class of low erosion risk varied from 13.36 to 15.22, mostly in the center-north area that gathers most of the UTRB. In contrast, higher potential areas for soil erosion (17.82–19.35) were restricted to the extreme south and southwest.

The soil erodibility map produced here clearly evidences the predominance of the very high class, determined by quartzarenic neossols and cambisols with 0.020–0.042 t $ha^{-1}.MJ^{-1}.mm^{-1}$ over 23.58% of the total area. The high class of erodibility was predominant with 40.27% of UTRB ranging from 0.016 to 0.020 t $ha^{-1}.MJ^{-1}.mm^{-1}$, comprising litholic neosols and plinthosols. The least restrictive class of low soil loss (0.002–0.011 t.ha-1.MJ-1.mm-1) gathered flat areas with planosols and gleysols in about 11.44%.

An average value of 5.19° or 9.23% of the third factor (*S*) was presented, however, the most important declivity class gathered almost 61% of the pixels distributed between 0° and 4.71°, called low in our soil model, and correlated to 0–3% and 3–8% of Embrapa's flat and smooth wavy relief, respectively. The second prominent class by area was the moderate with 31% of the pixels in a range from 4.71° to 10.54° of the slope. Extremes of mountainous (very high) represented just over 2% of the pixels.

The MSAVI high values are related to the low probability of soil loss and vice-versa. The map of Fig. 2d showed that approximately 76% of the area is included in moderate (41%) and high (35%) classes. The most fragile class ranged from 0.2 to −0.37, occupying approximately 14%.

The thirty-five assessments of soil erosion risk (USLE) were calculated based on the combination of factors and respective weights (Table 2). Altogether, gully and flat samples generated 18,808 and 10,222 pixels. The evaluation was carried out using a percentage of pixels in the most restrictive or very high associated with the flat or low probability of soil loss (Fig. S5). An isolated observation for the two parameters points out in test 13 (S0.25 + C0.75) with 71.15% of the pixels in the very high class for the gully samples. In the flat sample, test 21 (E1) showed 100% of pixels within the low range, nonetheless, the combination of samples brought test 11 (S0.25 + E0.75) with the highest average with 67.43% of pixels with low and/or very high erosive risk.

Test 30, in which all factors have the same 25% weight, was closest to the original USLE. However, the pixel average of 5.03% in the very high and low classes for the ravine and flat area samples did not accredit it for the final map of the erosive risk. The algebraic models in which the *R-factor* was predominant showed the worst outputs in the means, such as test 6 and tests 31 to 34. In summary, the spatial discrepancies between tests 6 and 11 can be verified in Fig. 3.

Table 3
Mean of vegetation and soil radiometric indices between September 2020 and April 2021.

Index	September 2020		Difference	April 2021		Difference
	high	low		high	low	
NDVI	0.38	0.53	−0.15	0.36	0.59	−0.23
TNDVI	0.40	0.53	−0.13	0.39	0.59	−0.20
EVI	0.38	0.53	−0.15	0.36	0.59	−0.23
SAVI	0.36	0.55	−0.19	0.37	0.61	−0.24
TSAVI	0.79	0.55	0.24	0.52	0.62	−0.10
MSAVI	0.37	0.55	−0.18	0.35	0.61	−0.26
BI	0.40	0.51	−0.11	0.38	0.44	−0.06
CI	0.53	0.49	0.04	0.67	0.47	0.20

3.3. Analysis of interventions in gullies

As expected, the UTRB presented many interventions led by the critical class 4 rate. Based on the land cover results in Table 3, we included the NDVI thresholds from the 2020 image of forest formation (>0.65), savanna (>0.57), and water (<0) to eliminate false positives (Fig. S6). Thus, the spatial algebra identified suitable locations for 3604 check dams and 1140 palisades (Fig. 4). The state of MS had 3598 or 76% of the total interventions, however, both states presented comparable densities of palisades and check dams per area, with 0.15 (MS) and 0.30 intervention/sq.km (MT).

The method for finding places for interventions was validated by the random sampler, with 95% CI, resulting in 360 and 296 samples for check dams and palisades, respectively. The validation indicates that 235 points or 65.28% of the check dam were assigned correctly considering the criteria described in item 2.4 (all sample points are shown in Table S4). On the other hand, palisade locations achieved a slightly lower percentage of 61.15%, representing 181 points. Fig. 5 depicts examples of the validation process with confirmed/unconfirmed points.

The method for the location of dam interventions showed promising accuracy, however, some drainage end points coincided with sandbanks in trunk rivers, such as the Coxim River in A2 in Fig. 5. Overall, the palisades were correlated with the environment ruled by the sloping terrain and unprotected soil, despite some non-exclusions by native gramineous (see example B2 on Fig. 5).

3.4. Integration of soil erosive risk, interventions, and CAR database

About 62.71% of the UTRB is composed of micro properties ranging from 0.24 to 279.9 ha, including rural settlements, whereas less than 10% represent large properties above 767.9 ha. In absolute terms, the area at high and very high risk of soil loss in large farms is almost 3 times the sum of micro, small and medium properties. However, the size of the property little influenced the average risk of soil erosion (see Fig. S7a), since all classes were close to 3 (high potential), and one-way ANOVA indicates no significant differences between classes of areas ($p = 0.33$). In comparison to the property's sizes, the features of AC, APP, and RL (Fig. S7b) were also equivalent with a mean erosive risk close to 3 but have significant differences by ANOVA ($p = 1.48E\text{-}7$), with RL distinct from AC and APP by Tukey's pairwise test ($p < 0.01$).

By linking the 4744 intervention points with polygons of 6571 properties of the SICAR database within the limits of the UTRB, we found that 8.3% of the dams and palisades were in micro properties, followed by 17.4 in small properties, 23.9% in medium size, and 50.3% inside large properties. In terms of internal polygons, AC has demanded 774 interventions, followed by RL with 1452 and APP with 1369 intervention points. The number of degraded lands in protected areas by legislation (RL and APP) was almost 50% higher than AC.

4. Discussion

4.1. Main drivers of soil loss in the region

The relative roles of land use and soil properties in shaping patterns of soil loss vary in different landscapes. Here we figured out that relief and erodibility are the main drivers. This finding calls into question the

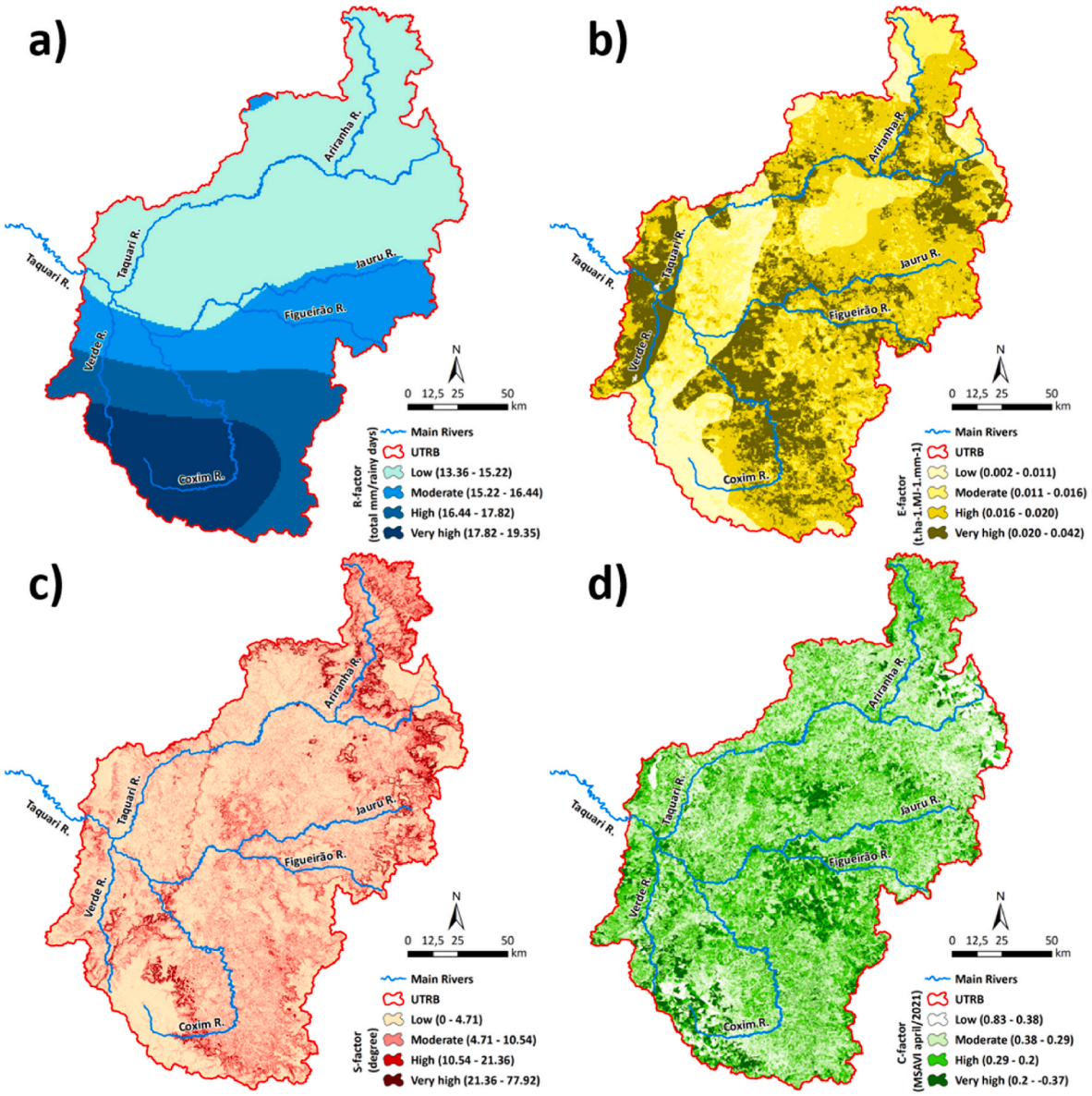

Fig. 2. The sequence of the factors for soil erosion risk evaluation: a) Rainfall index (R), b) Soil erodibility (E), c) Slope (S), and d) Land Use/Land Cover (C).

weight of anthropogenic changes in land use as the main factors of soil loss in the basin. On the other hand, recovery strategies directly involve farmers in the correct management of pastures added to the installation of mechanisms to stop the flow of eroding sediments. Our set of multi-criteria rules based on USLE principles, GIS algebra, and RS data allowed us to infer that about 65% of the UTRB area has a high risk of soil loss. Relief and soil properties are commonly highlighted as decisive factors in the erosion rate (Ruiz-Sinoga and Diaz, 2010; Lu et al., 2020), however, as a new contribution, we demonstrate that the soil cover factor does not seem to play the main role designed by Galdino et al. (2005), recently updated by Guerra et al. (2020). This may have occurred due to the fact that the most restrictive class of MSAVI belongs to portions with the total absence of vegetation (Sarparast et al., 2020), belonging to only 0.7% of the basin according to Mapbiomas 2019 (Souza et al., 2020). Even so, considering that the poorly managed pasture is the main villain of the erosive processes of the savanna pastures (Galdino et al., 2016; Colman et al., 2019), future studies maintaining our finest spatial resolution may add a possible correction to these effects by integrating the C-factor to the P-factor for erosion on a regional scale (Panagos et al., 2015).

4.2. Methodological challenges

Easy, fast, and free data for soil resource management is one of the bottlenecks for developing countries (Rosas and Gutierrez, 2020). As an open database, our algebra method exploited freely available resources and data. So, it can be a promising alternative for planning the territory of hydrographic basins already degraded by erosion, especially in developing countries (Mennecke and West Jr, 2001; Arabameri et al., 2019). Other advancements may provide for the inclusion of accurate relief models (see TanDEM-X performance at Boulton and Stokes, 2018). In addition, the analysis of soil spectral responses by RS would provide proxies for new pedological maps (Poppiel et al., 2019), which can contribute to the greater accuracy of the model. In the same way, the role of land cover, more precisely of native vegetation, could be aggregated in the form of historical data. That eliminates, for example, the focus on places with high potential for natural erosion, but the regeneration of vegetation cover has been mitigating the effect of rainfall on the soil (Zhang et al., 2004; Gahrizsangi et al., 2021).

The identification of locations with erosion for recovery interventions is the main outcome of our proposed spatial algebraic rules.

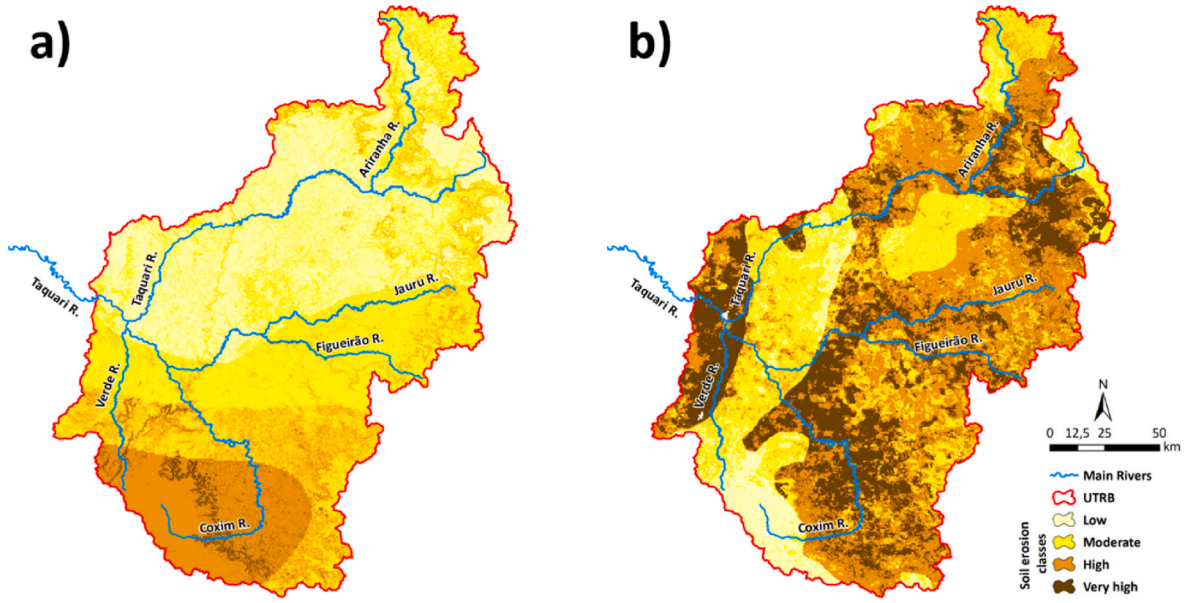

Fig. 3. Comparison map between the worst risk of soil erosion (a) of test 6 for 50% of *S-factor* and *R-factor*, and the best (b) of test 11 for 25% of *S-factor* and 75% of *E-factor*.

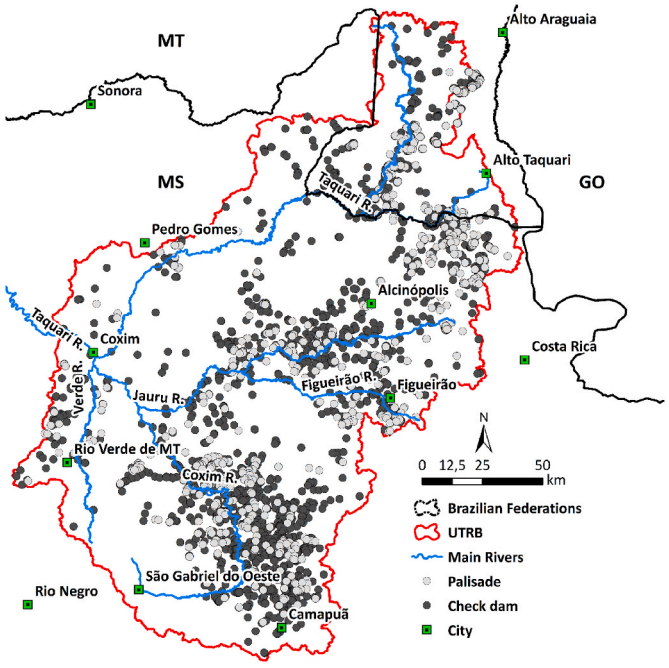

Fig. 4. Suitable areas for interventions with palisades and check dams detected in the UTRB.

We identified 4744 interventions, 76% of which are suitable for controlling dams. Proportionally, this is much higher than the 327 check dams reported by Rahmati et al. (2019), and 27 by Dash et al. (2021). According to our accuracy assessment, more than 60% of the palisades and check dams had locations related to severe erosive features, however new layers to false positive exclusion due to the influence of vegetation can be coupled in the method. By putting this into practice, we provide a basis for decision-makers to block more than half of the concentrated flow of sediment in the basin.

We emphasize that the zoning of interventions within erosions was only possible with the vectorization of the drainage lines through visual inspection. Although the current trend of applying machine learning algorithms dominates publications on the spatialization of erosive processes (Ghorbanzadeh et al., 2020) or the detection of ravine edges (Li et al., 2021), here we highlight the importance of human expertise on RS images analysis. In this sense, our algebra of selection and exclusion of false positives can be useful as an attribute for achieving more robust models (Minella et al., 2010), or even for integrating variables in GIS, such as distance to roads, lithology, slope curvatures, and topographic indices (Zabihi et al., 2018; Pourghasemi et al., 2020; Amiri and Pourghasemi, 2020), especially regarding the locations suitable for palisades, whose studies are still scarce.

Mapping the structures is the first step toward achieving basin sustainability. Unquestionably, check dams and palisades are effective in controlling sediment flow (Xu et al., 2020), however, this rule is limited to biophysical parameters alone and does not provide an integrated view. Studies have shown that for implementation it is necessary to take into account economic, social, and agrarian structure (Wynants et al., 2019).

4.3. Adding pieces to the puzzle: erosive risk, interventions, and agrarian structure

Based on our analysis of USLE parameters, we could identify priorities for erosion recovery interventions at a landscape scale in the Upper Taquari River Basin, however much work remains to translate it into action. In the real world, it is critical to assess cost, opportunities, economic, social, and policy aspects (Armsworth, 2014). By including information on the land structure of the region in our study, we were able to find that an erosion risk area on large properties is about 10 times greater than on micro properties. In this perspective, we agree with Stefanes et al. (2018) that the recovery of cattle pastures on large properties should be prioritized, as few properties already represent a gain in scale (area) to the renewal of the basin. Although we do not despise the micro properties, which lack technology and resources, this would represent a gain in participation and social engagement in relation to the conservation of natural resources (Tesfahunegn, 2019). Thus, we understand that the approaches are different and complementary.

Technically, large properties have an area available to carry out zoning between soil recovery (temporary stoppage) and agricultural production. In addition, they often have access to rural credit and machinery to support conservation activities (see an example in China's

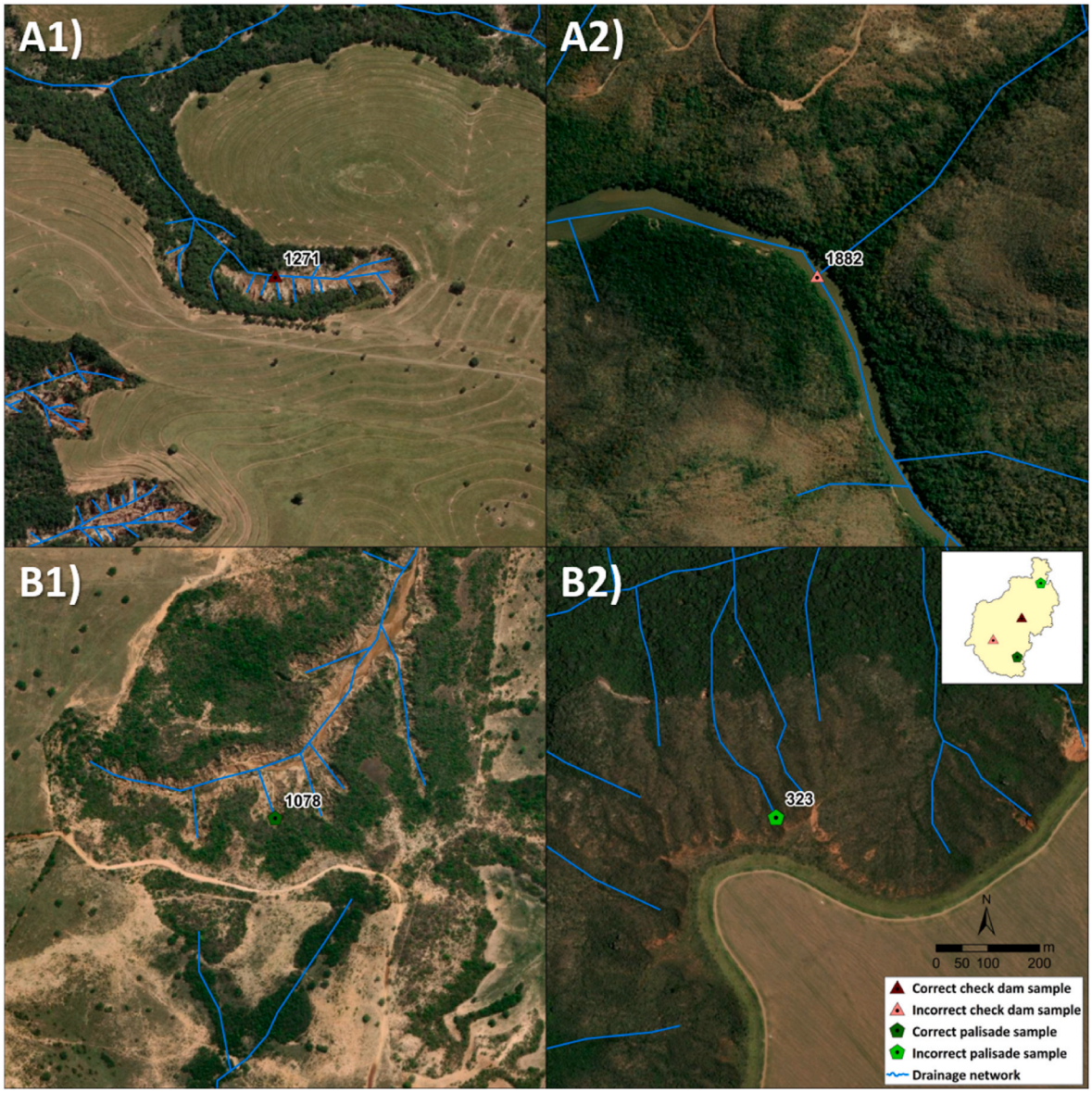

Fig. 5. Examples of check dams (A) and palisades (B) samples overlaid by a high-resolution orbital image available in the ArcGIS plugin. The numbers indicate those correctly (A1 and B1) and incorrectly (A2 and B2) determined by GIS algebra.

land arrangement by Ma et al., 2020). On the other hand, small properties do not have areas available for rotation, access to technology, and credit due to a lack of collateral registration (Carrer et al., 2020). Meanwhile, they may have the manpower to implement conservation practices, including operating machinery or collecting and planting seed species in gullies (Agidew and Singh, 2018; Schmidt et al., 2019). Therefore, given the dispersion of erosion points along the basin, we propose to divide the area into smaller projects, probably into micro catchments whose ecological trade-offs (Zhao et al., 2018) and cascading effects downstream on soil retention are measurable. (Sun et al. al., 2020). The regions of interest are also more favorable for the interaction between micro and large properties in the implementation of recovery actions (Toledo et al., 2018).

But where to start considering that active gullies on all properties are important for land restoration? The prioritization criteria may be constrained by a combination of costs, biodiversity conservation, and climate change mitigation (Strassburg et al., 2020). Indeed, setting restoration priorities is not a consensual issue. Overall, highly degraded areas are prioritized because they need urgent action (Lamb et al., 2005). However, a crescent number of studies also suggest that intermediate degraded areas should be prioritized because the costs and benefits are higher (Tambosi et al., 2014). According to Toledo et al. (2018), active restoration may be complemented by spontaneous regeneration in areas with less adverse conditions. In addition to the criteria already discussed we suggest to the decision makers an inclusion of a percentage of RL and APP surrounding the erosions to ranking gullies recovery. Basically, gullies permeated by vegetation can be rehabilitated a posteriori, according to their power of self-regeneration (Yang et al., 2018; Prieto et al., 2022). Erosion around the matrices (cattle) will likely be more costly due to the absence of native fragments but should be a priority to increase ecosystem connectivity (Tambosi et al., 2014; Blake et al., 2021).

The solutions for articulating interventions with the agrarian structure permeate the State's performance. We understand that large properties must be provoked by the government to achieve compliance with the Forest Code (Roitman et al., 2018; Stefanes et al., 2018), while structures in small and micro properties can be provided from specific public credit and payment programs for environmental services

(Brancalion et al., 2016).

5. Conclusion

The development of multi-criteria can be seen as a first step to planning the basin recovery. Areas of the high potential risk of soil loss in UTRB are evenly distributed between small and large properties, areas of anthropic use, and those reserved for conservation or preservation of natural resources. Similar status has been observed in pastures of savannas in tropical regions; therefore, the widespread degradation requires urgent prioritization for regional stabilization of tropical critical gullies.

The inclusion of agricultural information enriches the visualization of potential implementation opportunities. The weaknesses of one ownership group can be addressed by the strengths of others, as in a collaborative action system. However, the State government is instrumental in invoking, especially with the creation of specific financial resources rooted in public policies for groups of fragile properties in compliance with the Forest Code through the CAR.

Funding

This research did not receive any specific grant from funding agencies in the public, commercial, or not-for-profit sectors.

Credit author statement

Author 1: Louzada, Rômullo Oliveira: Conceptualization, Methodology, Data curation, Writing-Original draft preparation. **Author 2:** Bergier, Ivan: Conceptualization, Methodology, Supervision, Writing-Reviewing and Editing. **Author 3:** Diniz, Juliana Maria Ferreira de: Methodology, Writing- Reviewing and Editing. **Author 4:** Guerra, Angélica: Writing- Reviewing and Editing. **Author 5:** Roque, Fabio Oliveira: Supervision, Writing- Reviewing and Editing.

Declaration of competing interest

The authors declare that they have no known competing financial interests or personal relationships that could have appeared to influence the work reported in this paper.

Data availability

The authors do not have permission to share data.

Appendix A. Supplementary data

Supplementary data to this article can be found online at https://doi.org/10.1016/j.jenvman.2022.116219.

References

Abdulkareem, J.H., Pradhan, B., Sulaiman, W.N.A., Jamil, N.R., 2019. Prediction of spatial soil loss impacted by long-term land-use/land-cover change in a tropical watershed. Geosci. Front. 10 (2), 389–403. https://doi.org/10.1016/j.gsf.2017.10.010.

Agidew, A.-m. A., Singh, K.N., 2018. Factors affecting farmers' participation in watershed management programs in the Northeastern highlands of Ethiopia: a case study in the Teleyayen sub-watershed. Ecolog. Process. 7 (1), 15. https://doi.org/10.1186/s13717-018-0128-6.

Alewell, C., Borrelli, P., Meusburger, K., Panagos, P., 2019. Using the USLE: chances, challenges, and limitations of soil erosion modelling. Int. Soil Water Conserv. Res. 7 (3), 203–225. https://doi.org/10.1016/j.iswcr.2019.05.004.

Amiri, M., Pourghasemi, H.R., 2020. Mapping and preparing a susceptibility map of gully erosion using the MARS model. In: Shit, P.K., Pourghasemi, H.R., Bhunia, G.S. (Eds.), Gully Erosion Studies from India and Surrounding Regions. Cham: Springer International Publishing, pp. 405–413.

Arabameri, A., Pradhan, B., Rezaei, K., 2019. Spatial prediction of gully erosion using ALOS PALSAR data and ensemble bivariate and data mining models. Geosci. J. 23 (4), 669–686. https://doi.org/10.1007/s12303-018-0067-3.

Armsworth, P.R., 2014. Inclusion of costs in conservation planning depends on limited datasets and hopeful assumptions. Ann. N. Y. Acad. Sci. 1322 (1), 61–76. https://doi.org/10.1111/nyas.12455.

Assine, M.L., 2005. River avulsions on the Taquari megafan, Pantanal wetland, Brazil. Geomorphology 70 (3), 357–371. https://doi.org/10.1016/j.geomorph.2005.02.013.

Baret, F., Guyot, G., 1991. Potentials and limits of vegetation indices for LAI and APAR assessment. Rem. Sens. Environ. 35 (2), 161–173. https://doi.org/10.1016/0034-4257(91)90009-U.

Beller, E.E., Spotswood, E.N., Robinson, A.H., Anderson, M.G., Higgs, E.S., Hobbs, R.J., Grossinger, R.M., 2019. Building ecological resilience in highly modified landscapes. Bioscience 69 (1), 80–92. https://doi.org/10.1093/biosci/biy117.

Bergier, I., 2013. Effects of highland land-use over lowlands of the Brazilian Pantanal. Sci. Total Environ. 463–464, 1060–1066. https://doi.org/10.1016/j.scitotenv.2013.06.036.

Bergier, I., Assine, M.L., McGlue, M.M., Alho, C.J.R., Silva, A., Guerreiro, R.L., Carvalho, J.C., 2018. Amazon rainforest modulation of water security in the Pantanal wetland. Sci. Total Environ. 619–620, 1116–1125. https://doi.org/10.1016/j.scitotenv.2017.11.163.

Blake, W.H., Kelly, C., Wynants, M., Patrick, A., Lewin, S., Lawson, J., Ndakidemi, P., 2021. Integrating land-water-people connectivity concepts across disciplines for co-design of soil erosion solutions. Land Degrad. Dev. 32 (12), 3415–3430. https://doi.org/10.1002/ldr.3791.

Boardman, J., Vandaele, K., Evans, R., Foster, I.D.L., 2019. Off-site impacts of soil erosion and runoff: why connectivity is more important than erosion rates. Soil Use Manag. 35 (2), 245–256. https://doi.org/10.1111/sum.12496.

Borrelli, P., Robinson, D.A., Panagos, P., Lugato, E., Yang, J.E., Alewell, C., Ballabio, C., 2020. Land use and climate change impacts on global soil erosion by water (2015-2070). Proc. Natl. Acad. Sci. USA 117 (36), 21994. https://doi.org/10.1073/pnas.2001403117.

Boulton, S.J., Stokes, M., 2018. Which DEM is best for analyzing fluvial landscape development in mountainous terrains? Geomorphology 310, 168–187. https://doi.org/10.1016/j.geomorph.2018.03.002.

Brancalion, P.H.S., Garcia, L.C., Loyola, R., Rodrigues, R.R., Pillar, V.D., Lewinsohn, T. M., 2016. A critical analysis of the Native Vegetation Protection Law of Brazil (2012): updates and ongoing initiatives. Natureza & Conservação 14, 1–15. https://doi.org/10.1016/j.ncon.2016.03.003.

Carrer, M.J., Maia, A.G., de Mello Brandão Vinholis, M., de Souza Filho, H.M., 2020. Assessing the effectiveness of rural credit policy on the adoption of integrated crop-livestock systems in Brazil. Land Use Pol. 92, 104468 https://doi.org/10.1016/j.landusepol.2020.104468.

Chen, S., Zha, X., Bai, Y., Wang, L., 2019. Evaluation of soil erosion vulnerability on the basis of exposure, sensitivity, and adaptive capacity: a case study in the Zhuxi watershed, Changting, Fujian Province, Southern China. Catena 177, 57–69. https://doi.org/10.1016/j.catena.2019.01.036.

Colman, C.B., Oliveira, P.T.S., Almagro, A., Soares-Filho, B.S., Rodrigues, D.B.B., 2019. Effects of climate and land-cover changes on soil erosion in Brazilian pantanal. Sustainability 11 (24), 7053. https://doi.org/10.3390/su11247053.

Dash, S.S., Paul, J.C., Panigrahi, B., 2021. Assessing soil erosion vulnerability and locating suitable conservation structures for agricultural planning using GIS - a case study of Altuma catchment of Brahmani river Basin, Odisha, India. Arabian J. Geosci. 14 (21), 2201. https://doi.org/10.1007/s12517-021-08493-2.

Dominati, E., Patterson, M., Mackay, A., 2010. A framework for classifying and quantifying the natural capital and ecosystem services of soils. Ecol. Econ. 69 (9), 1858–1868. https://doi.org/10.1016/j.ecolecon.2010.05.002.

Durigon, V.L., Carvalho, D.F., Antunes, M.A.H., Oliveira, P.T.S., Fernandes, M.M., 2014. NDVI time series for monitoring RUSLE cover management factor in a tropical watershed. Int. J. Rem. Sens. 35 (2), 441–453. https://doi.org/10.1080/01431161.2013.871081.

El Jazouli, A., Barakat, A., Ghafiri, A., El Moutaki, S., Ettaqy, A., Khellouk, R., 2017. Soil erosion modeled with USLE, GIS, and remote sensing: a case study of Ikkour watershed in Middle Atlas (Morocco). Geosci. Lett. 4 https://doi.org/10.1186/s40562-017-0091-6.

Escadafal, R., 1989. Remote sensing of arid soil surface color with Landsat thematic mapper. Adv. Space Res. 9 (1), 159–163. https://doi.org/10.1016/0273-1177(89)90481-X.

Ewunetu, A., Simane, B., Teferi, E., Zaitchik, B.F., 2021. Mapping and quantifying comprehensive land degradation status using spatial multicriteria evaluation technique in the headwaters area of upper blue nile river. Sustainability 13 (4). https://doi.org/10.3390/su13042244.

Filizola, H.F., Almeida Filho, G.S., Souza, M.D., Gomes, M.A.F., 2011. Controle dos processos erosivos lineares (ravinas e voçorocas) em áreas de solos arenosos. Embrapa Meio Ambiente, Jaguariúna, p. 7.

Gahrizsangi, H.S., Eslamian, S., Dalezios, N.R., Blanta, A., Madadi, M., 2021. Vegetation Advantages for Water and Soil Conservation. Handbook of Water Harvesting and Conservation, pp. 321–336. https://doi.org/10.1002/9781119478911.ch21.

Galdino, S., Vieira, L.M., Pellegrin, L.A., 2005. Impactos ambientais e socioeconômicos na Bacia do Rio Taquari-Pantanal: Corumbá. Embrapa Pantanal, 2005.

Galdino, S., Sano, E.E., Andrade, R.G., Grego, C.R., Nogueira, S.F., Bragantini, C., Flosi, A.H.G., 2016. Large-scale modeling of soil erosion with RUSLE for conservationist planning of degraded cultivated Brazilian pastures. Land Degrad. Dev. 27 (3), 773–784. https://doi.org/10.1002/ldr.2414.

Gao, J., Wang, H., 2019. Temporal analysis on quantitative attribution of karst soil erosion: a case study of a peak-cluster depression basin in Southwest China. Catena 172, 369–377. https://doi.org/10.1016/j.catena.2018.08.035.

García-Ruiz, J.M., Beguería, S., Lana-Renault, N., Nadal-Romero, E., Cerdà, A., 2017. Ongoing and emerging questions in water erosion studies. Land Degrad. Dev. 28 (1), 5–21. https://doi.org/10.1002/ldr.2641.

Ghorbanzadeh, O., Shahabi, H., Mirchooli, F., Valizadeh Kamran, K., Lim, S., Aryal, J., Blaschke, T., 2020. Gully erosion susceptibility mapping (GESM) using machine learning methods optimized by the multi-collinearity analysis and K-fold cross-validation. Geomatics, Nat. Hazards Risk 11 (1), 1653–1678. https://doi.org/10.1080/19475705.2020.1810138.

Godoi, R.d.F., Rodrigues, D.B.B., Borrelli, P., Oliveira, P.T.S., 2021. High-resolution soil erodibility map of Brazil. Sci. Total Environ. 781, 146673 https://doi.org/10.1016/j.scitotenv.2021.146673.

Guerra, A., Oliveira, P.T. S.d., Roque, F.d.O., Rosa, I.M.D., Ochoa-Quintero, J.M., Guariento, R.D., Garcia, L.C., 2020. The importance of Legal Reserves for protecting the Pantanal biome and preventing agricultural losses. J. Environ. Manag. 260, 110128 https://doi.org/10.1016/j.jenvman.2020.110128.

Huete, A.R., 1988. A soil-adjusted vegetation index (SAVI). Rem. Sens. Environ. 25 (3), 295–309. https://doi.org/10.1016/0034-4257(88)90106-X.

Jiang, Z., Huete, A.R., Didan, K., Miura, T., 2008. Development of a two-band enhanced vegetation index without a blue band. Rem. Sens. Environ. 112 (10), 3833–3845. https://doi.org/10.1016/j.rse.2008.06.006.

Keesstra, S.D., Bouma, J., Wallinga, J., Tittonell, P., Smith, P., Cerdà, A., Fresco, L.O., 2016. The significance of soils and soil science towards realization of the United Nations Sustainable Development Goals. SOIL 2 (2), 111–128. https://doi.org/10.5194/soil-2-111-2016.

Lamb, D., Erskine, P.D., Parrotta, J.A., 2005. Restoration of degraded tropical forest landscapes. Science 310 (5754), 1628–1632. https://doi.org/10.1126/science.1111773.

Laurencelle, J., Logan, T., Gens, R., 2015. ASF Radiometrically Terrain Corrected ALOS PALSAR Products. Alaska Satellite Facility, Fairbanks, Alaska.

Li, S., Xiong, L., Hu, G., Dang, W., Tang, G., Strobl, J., 2021. Extracting check dam areas from high-resolution imagery based on the integration of object-based image analysis and deep learning. Land Degrad. Dev. 32 (7), 2303–2317. https://doi.org/10.1002/ldr.3908.

Libonati, R., DaCamara, C.C., Peres, L.F., Sander de Carvalho, L.A., Garcia, L.C., 2020. Rescue Brazil's Burning Pantanal Wetlands, vol. 588, pp. 217–219. https://doi.org/10.1038/d41586-020-03464-1.

Lo, E.L., Yeager, K.M., Bergier, I., Domingos-Luz, L., Silva, A., McGlue, M.M., 2022. Sediment infill of tropical floodplain lakes: rates, controls, and implications for ecosystem services. Front. Earth Sci. 10 https://doi.org/10.3389/feart.2022.875919.

Louzada, R.O., Bergier, I., Assine, M.L., 2020. Landscape changes in avulsive river systems: case study of Taquari River on Brazilian Pantanal wetlands. Sci. Total Environ. 723, 138067 https://doi.org/10.1016/j.scitotenv.2020.138067.

Louzada, R.O., Bergier, I., Roque, F.O., McGlue, M.M., Silva, A., Assine, M.L., 2021. Avulsions drive ecosystem services and economic changes in the Brazilian Pantanal wetlands. Curr. Res. Environ. Sustain. 3, 100057 https://doi.org/10.1016/j.crsust.2021.100057.

Lu, S., Liu, B., Hu, Y., Fu, S., Cao, Q., Shi, Y., Huang, T., 2020. Soil erosion topographic factor (LS): accuracy calculated from different data sources. Catena 187, 104334. https://doi.org/10.1016/j.catena.2019.104334.

Machado, R.L., Resende, A.S., Campello, E.F., Menezes, C.E.G., Souza, C.M., Franco, A. A., 2006. Recuperação de voçorocas em áreas rurais. In: Embrapa Agrobiologia-Sistema de Produção. Embrapa Agrobiologia, Seropédica, p. 63.

Marengo, J.A., Oliveira, G.S., Alves, L.M., 2015. Climate change scenarios in the Pantanal. In: Dynamics of the Pantanal Wetland in South America. Springer, pp. 227–238.

Mathieu, R., Pouget, M., Cervelle, B., Escadafal, R., 1998. Relationships between satellite-based radiometric indices simulated using laboratory reflectance data and typic soil color of an arid environment. Rem. Sens. Environ. 66 (1), 17–28. https://doi.org/10.1016/S0034-4257(98)00030-3.

Mennecke, B.E., West Jr., L.A., 2001. Geographic information systems in developing countries: issues in data collection, implementation and management. J. Global Inf. Manag. 9 (4), 44–54. https://doi.org/10.4018/jgim.2001100103.

Minella, J.P.G., Merten, G.H., Reichert, J.M., Cassol, E.A., 2010. Processos e modelagem da erosão: da parcela à bacia hidrográfica. In: Manejo e conservação do solo e da água no contexto das mudanças ambientais. Embrapa Solos, Rio de Janeiro, pp. 105–135.

Norris, J.E., Stokes, A., Mickovski, S.B., Cammeraat, E., Van Beek, R., Nicoll, B.C., Achim, A., 2008. Slope Stability and Erosion Control: Ecotechnological Solutions. Springer Science & Business Media.

Panagos, P., Borrelli, P., Meusburger, K., van der Zanden, E.H., Poesen, J., Alewell, C., 2015. Modelling the effect of support practices (P-factor) on the reduction of soil erosion by water at European scale. Environ. Sci. Pol. 51, 23–34. https://doi.org/10.1016/j.envsci.2015.03.012.

Pena, S.B., Abreu, M.M., Magalhães, M.R., Cortez, N., 2020. Water erosion aspects of land degradation neutrality to landscape planning tools at national scale. Geoderma 363, 114093. https://doi.org/10.1016/j.geoderma.2019.114093.

Poppiel, R.R., Lacerda, M.P.C., Demattê, J.A.M., Oliveira, M.P., Gallo, B.C., Safanelli, J. L., 2019. Pedology and soil class mapping from proximal and remote sensed data. Geoderma 348, 189–206. https://doi.org/10.1016/j.geoderma.2019.04.028.

Pourghasemi, H.R., Yousefi, S., Sadhasivam, N., Eskandari, S., 2020. Assessing, mapping, and optimizing the locations of sediment control check dams construction. Sci. Total Environ. 739, 139954 https://doi.org/10.1016/j.scitotenv.2020.139954.

Prieto, P.V., Bukoski, J.J., Barros, F.S.M., Beyer, H.L., Iribarrem, A., Brancalion, P.H.S., Crouzeilles, R., 2022. Predicting landscape-scale biodiversity recovery by natural tropical forest regrowth. Conserv. Biol. 36 (3), e13842 https://doi.org/10.1111/cobi.13842.

Pruski, F.F., 2006. Conservação de solo e água: práticas mecânicas para o controle da erosão hídrica. Universidade Federal de Viçosa, Viçosa.

Qi, J., Chehbouni, A., Huete, A.R., Kerr, Y.H., Sorooshian, S., 1994. A modified soil adjusted vegetation index. Rem. Sens. Environ. 48 (2), 119–126. https://doi.org/10.1016/0034-4257(94)90134-1.

Rahmati, O., Kalantari, Z., Samadi, M., Uuemaa, E., Moghaddam, D.D., Nalivan, O.A., Tien Bui, D., 2019. GIS-based site selection for check dams in watersheds: considering geomorphometric and topo-hydrological factors. Sustainability 11 (20). https://doi.org/10.3390/su11205639.

Rodrigues, S.C., 2018. Some practices of gully rehabilitation in Central Brazil. In: Ravine Lands: Greening for Livelihood and Environmental Security. Springer, pp. 183–193.

Roitman, I., Cardoso Galli Vieira, L., Baiocchi Jacobson, T.K., da Cunha Bustamante, M. M., Silva Marcondes, N.J., Cury, K., Avila, M.L., 2018. Rural Environmental Registry: an innovative model for land-use and environmental policies. Land Use Pol. 76, 95–102. https://doi.org/10.1016/j.landusepol.2018.04.037.

Roque, F.O., Ochoa-Quintero, J., Ribeiro, D.B., Sugai, L.S.M., Costa-Pereira, R., Lourival, R., Bino, G., 2016. Upland Habitat Loss as a Threat to Pantanal Wetlands, vol. 30, pp. 1131–1134. https://doi.org/10.1111/cobi.12713, 5.

Roque, F.d.O., Guerra, A., Johnson, M., Padovani, C., Corbi, J., Covich, A.P., Yon, L., 2021. Simulating land use changes, sediment yields, and pesticide use in the Upper Paraguay River Basin: implications for conservation of the Pantanal wetland. Agric. Ecosyst. Environ. 314, 107405 https://doi.org/10.1016/j.agee.2021.107405.

Rosas, M.A., Gutierrez, R.R., 2020. Assessing soil erosion risk at national scale in developing countries: the technical challenges, a proposed methodology, and a case history. Sci. Total Environ. 703, 135474 https://doi.org/10.1016/j.scitotenv.2019.135474.

Rouse, J.W., Haas, R.H., Schell, J.A., Deering, D.W., Harlan, J.C., 1973. Monitoring the Vernal Advancement and Retrogradation (Green Wave Effect) of Natural Vegetation. NASA/GSFC Type III Final Report, Greenbelt, Md, p. 371.

Ruiz-Sinoga, J.D., Diaz, A.R., 2010. Soil degradation factors along a Mediterranean pluviometric gradient in Southern Spain. Geomorphology 118 (3), 359–368. https://doi.org/10.1016/j.geomorph.2010.02.003.

Sarparast, M., Ownegh, M., Sepehr, A., 2020. Evaluating the impacts of combating-action programs on desertification hazard trends: a case study of Taybad-Bakharz region, northeastern Iran. Environ. Sustain. Indicat. 7, 100043 https://doi.org/10.1016/j.indic.2020.100043.

Schmidt, I.B., de Urzedo, D.I., Piña-Rodrigues, F.C.M., Vieira, D.L.M., de Rezende, G.M., Sampaio, A.B., Junqueira, R.G.P., 2019. Community-based native seed production for restoration in Brazil – the role of science and policy. Plant Biol. 21 (3), 389–397. https://doi.org/10.1111/plb.12842.

Seixas, C.D.S., Godoy, C.V., 2007. Vazio sanitário: panorama nacional e medidas de monitoramento. In: Paper presented at the simpósio brasileiro de ferrugem asiática da soja, Londrina.

Senanayake, S., Pradhan, B., Huete, A., Brennan, J., 2020. A review on assessing and mapping soil erosion hazard using geo-informatics technology for farming system management. Rem. Sens. 12 (24) https://doi.org/10.3390/rs12244063.

Senseman, G.M., Bagley, C.F., Tweddale, S.A., 1996. Correlation of rangeland cover measures to satellite-imagery-derived vegetation indices. Geocarto Int. 11 (3), 29–38. https://doi.org/10.1080/10106049609354546.

Sepuru, T.K., Dube, T., 2018. An appraisal on the progress of remote sensing applications in soil erosion mapping and monitoring. Remote Sens. Appl.: Soc. Environ. 9, 1–9. https://doi.org/10.1016/j.rsase.2017.10.005.

Silva, P.S., Bastos, A., Libonati, R., Rodrigues, J.A., DaCamara, C.C., 2019. Impacts of the 1.5 °C global warming target on future burned area in the Brazilian Cerrado. For. Ecol. Manag. 446, 193–203. https://doi.org/10.1016/j.foreco.2019.05.047.

Souza, C.M., Shimbo, Z., J, Rosa, M.R., Parente, L.L., A Alencar, A., Rudorff, B.F.T., Azevedo, T., 2020. Reconstructing three decades of land use and land cover changes in Brazilian biomes with landsat. Archive and Earth Engine 12 (17), 2735. https://doi.org/10.3390/rs12172735.

Stefanes, M., Roque, F.d.O., Lourival, R., Melo, I., Renaud, P.C., Quintero, J.M.O., 2018. Property size drives differences in forest code compliance in the Brazilian Cerrado. Land Use Pol. 75, 43–49. https://doi.org/10.1016/j.landusepol.2018.03.022.

Strassburg, B.B.N., Iribarrem, A., Beyer, H.L., Cordeiro, C.L., Crouzeilles, R., Jakovac, C. C., Visconti, P., 2020. Global priority areas for ecosystem restoration. Nature 586 (7831), 724–729. https://doi.org/10.1038/s41586-020-2784-9.

Sun, P., Wu, Y., Gao, J., Yao, Y., Zhao, F., Lei, X., Qiu, L., 2020. Shifts of sediment transport regime caused by ecological restoration in the Middle Yellow River Basin. Sci. Total Environ. 698, 134261 https://doi.org/10.1016/j.scitotenv.2019.134261.

Tambosi, L.R., Martensen, A.C., Ribeiro, M.C., Metzger, J.P., 2014. A framework to optimize biodiversity restoration efforts based on habitat amount and landscape connectivity. Restor. Ecol. 22 (2), 169–177. https://doi.org/10.1111/rec.12049.

Tardio, G., B M S, Alexia, S., Sanjaya, D., 2017. Bamboo structures as a resilient erosion control measure. Proc. Inst. Civ. Eng.: Forensic Eng. 170 (2), 72–83. https://doi.org/10.1680/jfoen.16.00033.

Telles, T.S., Dechen, S.C.F., Souza, L.G. A.d., Guimarães, M.d.F., 2013. Valuation and assessment of soil erosion costs. Sci. Agric. 70, 209–216. https://doi.org/10.1590/S0103-90162013000300010.

Tesfahunegn, G.B., 2019. Farmers' perception on land degradation in northern Ethiopia: implication for developing sustainable land management. Soc. Sci. J. 56 (2), 268–287. https://doi.org/10.1016/j.soscij.2018.07.004.

Thielen, D., Schuchmann, K.-L., Ramoni-Perazzi, P., Marquez, M., Rojas, W., Quintero, J. I., Marques, M.I., 2020. Quo vadis Pantanal? Expected precipitation extremes and drought dynamics from changing sea surface temperature. PLoS One 15 (1), e0227437. https://doi.org/10.1371/journal.pone.0227437.

Toledo, R.M., Santos, R.F., Verheyen, K., Perring, M.P., 2018. Ecological restoration efforts in tropical rural landscapes: challenges and policy implications in a highly degraded region. Land Use Pol. 75, 486–493. https://doi.org/10.1016/j.landusepol.2018.03.053.

Wischmeier, W.H., Smith, D.D., 1965. Predicting Rainfall-Erosion Losses from Cropland East of the Rocky Mountains. Agricultural Research Service. US Department of Agriculture.

Wuepper, D., Borrelli, P., Finger, R., 2020. Countries and the global rate of soil erosion. Nat. Sustain. 3 (1), 51–55. https://doi.org/10.1038/s41893-019-0438-4.

Wynants, M., Kelly, C., Mtei, K., Munishi, L., Patrick, A., Rabinovich, A., Ndakidemi, P., 2019. Drivers of increased soil erosion in East Africa's agro-pastoral systems: changing interactions between the social, economic and natural domains. Reg. Environ. Change 19 (7), 1909–1921. https://doi.org/10.1007/s10113-019-01520-9.

Xu, X., Zhu, T., Zhang, H., Gao, L., 2020. Sediment-storage effects of check-dam system in the small watershed. In: Experimental Erosion. Springer, pp. 113–139.

Yang, Y., Wang, L., Yang, Z., Xu, C., Xie, J., Chen, G., Lin, T.-C., 2018. Large ecosystem service benefits of assisted natural regeneration. J. Geophys. Res.: Biogeosciences 123 (2), 676–687. https://doi.org/10.1002/2017JG004267.

Yesuph, A.Y., Dagnew, A.B., 2019. Soil erosion mapping and severity analysis based on RUSLE model and local perception in the Beshillo Catchment of the Blue Nile Basin, Ethiopia. Environ. Syst. Res. 8 (1), 17. https://doi.org/10.1186/s40068-019-0145-1.

Zabihi, M., Mirchooli, F., Motevalli, A., Khaledi Darvishan, A., Pourghasemi, H.R., Zakeri, M.A., Sadighi, F., 2018. Spatial modelling of gully erosion in Mazandaran Province, northern Iran. Catena 161, 1–13. https://doi.org/10.1016/j.catena.2017.10.010.

Zhang, B., Yang, Y.-s., Zepp, H., 2004. Effect of vegetation restoration on soil and water erosion and nutrient losses of a severely eroded clayey Plinthudult in southeastern China. Catena 57 (1), 77–90. https://doi.org/10.1016/j.catena.2003.07.001.

Zhao, M., Peng, J., Liu, Y., Li, T., Wang, Y., 2018. Mapping watershed-level ecosystem service bundles in the pearl river delta, China. Ecol. Econ. 152, 106–117. https://doi.org/10.1016/j.ecolecon.2018.04.023.